Finite-size effects on coherent folded acoustic phonons in GaAs/AlAs superlattices

2002 J. Phys.: Condens. Matter 14 L103

(http://iopscience.iop.org/0953-8984/14/4/106)

INSTITUTE OF PHYSICS PUBLISHING JOURNAL OF PHYSICS: CONDENSED MATTER

J. Phys.: Condens. Matter **14** (2002) L103–L109 PII: S0953-8984(02)31287-6

LETTER TO THE EDITOR

Finite-size effects on coherent folded acoustic phonons in GaAs/AlAs superlattices

K Mizoguchi, H Takeuchi, T Hino and M Nakayama

Department of Applied Physics, Osaka City University, 3-3-138 Sugimoto, Sumiyoshi-ku, Osaka 558-8585, Japan

E-mail: mizoguch@a-phys.eng.osaka-cu.ac.jp

Received 27 November 2001
Published 18 January 2002
Online at stacks.iop.org/JPhysCM/14/L103

Abstract

We have investigated dynamical properties of coherent folded longitudinal acoustic (FLA) phonons generated in $(GaAs)_{10}(AlAs)_{10}$ superlattices (SLs) with 20, 100 and 195 periods. In the time-domain signals of the SL with 20 periods, the coherent FLA phonon mode with the Raman-inactive B_2 symmetry at the Brillouin zone centre, which is not observed in the SLs with more than 100 periods, is detected in addition to the Raman-active modes with the A_1 symmetry at and near the zone centre. The appearance of the B_2 mode is caused by the break of the mode symmetry due to the finiteness of the total number of periods. Moreover, it is found that the bandwidths of the coherent FLA phonon modes observed in the Fourier transform spectra depend on the finiteness of periodicity and the wavevector, which is discussed from the aspect of the relaxation of the wavevector conservation and the propagation of the phonon wavepacket through the SL region.

A time-domain spectroscopy with femtosecond laser pulses is a useful technique to investigate the dynamics of the phonon excited in materials, such as semimetals, semiconductors and semiconductor superlattices (SLs) [1–7]. To date, there are several reports on the propagation of coherent longitudinal acoustic (LA) phonons emitted from a single quantum well [3] and generated in SLs [5, 6] using a one-colour (1C) or two-colour (2C) pump–probe technique. SLs are better suited than bulk crystals for the investigation of the phonon dynamics because of the controllability of the periodic structure. The propagating and standing phonon waves in GaAs/AlAs SLs are simultaneously observed by using the 1C pump–probe technique: coherent folded longitudinal acoustic (FLA) phonons with the A_1 symmetry in the SLs have been observed at and near the Brillouin zone centre [4–7]. These coherent FLA phonon modes at and near the zone centre correspond to the phonon modes observed in the configuration of forward and backward Raman scattering, respectively. Recently, we reported that the wavevector of the coherent FLA phonons observed by using the pump–probe technique obeys the Raman

selection rule at the detection process [6]. In the study for coherent FLA phonons [4–7], SL samples used had more than 100 periods and were treated as an infinite periodic structure. We note that no attention has been paid to effects of finiteness along a growth direction on coherent FLA phonons. The study of the finite-size effect on the coherent FLA phonons is a very interesting subject from the viewpoint of the phonon dynamics in a spatially limited region.

Finite-size effects on Raman scattering have been investigated in microcrystals [8–10], ion-implanted semiconductors [11] and SLs [12]. For an ideal crystal, a conservation of photon and phonon momentums allows only the phonon wavevector at $q = k_s$, where q and k_s are phonon and scattering wavevectors, respectively. For a semiconductor microcrystal and a SL with a limited periodicity, the finiteness of the crystal size or the periodicity leads to a frequency shift and broadening of the first-order Raman peak through a relaxation of the q-selection rule [9–12]. As mentioned above, the similarity between the coherent phonon and Raman modes expects us to observe the broadening of the coherent phonon modes generated in a restricted region by using the pump–probe technique.

This letter reports the time-resolved study of the coherent FLA phonons generated in the $(GaAs)_{10}(AlAs)_{10}$ SLs with 20, 100 and 195 periods, where the subscripts denote the monolayer numbers of GaAs or AlAs (thickness of one monlayer is equal to 0.283 nm). The Fourier transform (FT) spectra of the time-domain signals in the SLs with 100 and 195 periods show the FLA phonon modes with only the A_1 symmetry at and near the zone centre, which are allowed on Raman scattering. In contrast, the FT spectrum in the SL with 20 periods exhibits obviously the FLA phonon mode with the B_2 symmetry at the zone centre, which is forbidden in principle on the Raman scattering, in addition to the modes with the A_1 symmetry. The appearance of the FLA phonon with the B_2 symmetry will originate from the break of the mode symmetry due to the finite-size effect. The FLA phonon modes in the SL with 20 periods are broader than those in the SLs with 100 and 195 periods. We discuss the period-number dependence of the bandwidth of the FLA phonons observed in the FT spectra from the aspect of the relaxation of the wavevector conservation and the propagation of the phonon wavepacket through the SL layer.

The samples of $(GaAs)_{10}(AlAs)_{10}$ SLs with 20, 100 and 195 periods were grown on a (001) GaAs substrate by molecular beam epitaxy (MBE). Hereafter, we will call these three samples '$(10, 10)_{20}$ SL', '$(10, 10)_{100}$ SL' and '$(10, 10)_{195}$ SL', respectively. Reflection-type pump–probe measurements were performed at room temperature by using a mode-locked Ti:sapphire pulse laser delivering about 100 fs pulses. The 1C pump–probe measurements were performed using the fundamental laser light with the wavelength of 720 nm tuned closely to the first interband transition of the SLs, which was determined by a photoreflectance experiment. In the 2C pump–probe measurement, the probe and pump beams were the fundamental laser light with the wavelength of 720 nm and its second-harmonic light with the wavelength of 360 nm, respectively. The time delay of the probe beam was adjusted by a variable optical delay line. The optical path of the pump beam was modulated by a shaker. The time derivative of the reflectivity change, $\partial(\Delta R/R_0)/\partial t$, was recorded in order to highlight the oscillatory component. We extracted only the signals of the FLA phonons by subtracting a slowly varying background due to the sound wave.

Figure 1 shows the time derivative signals of reflectivity changes in the SLs with 20 and 195 periods obtained by using the 1C and 2C pump–probe techniques. In the $(10, 10)_{195}$ SL, the time-domain signals obtained by the 1C and 2C pump–probe techniques show the oscillatory structures with beats in the time range more than 100 ps. The main period of the oscillations in both the 1C and 2C pump–probe signals is about 1.1 ps. The 1C pump–probe signal gradually decays, while the amplitude of the beat signal obtained by the 2C pump–probe

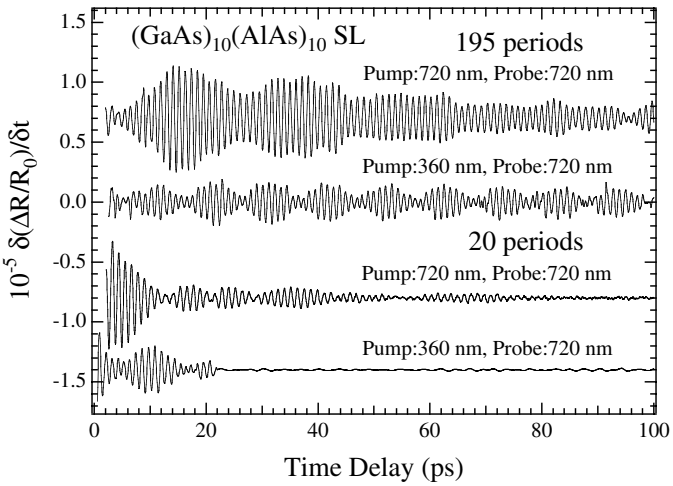

Figure 1. Oscillatory parts of the time-resolved reflectivity changes of the (10, 10) SLs with 195 and 20 periods observed by using 1C and 2C pump–probe techniques.

technique hardly changes. We have also observed the 1C and 2C pump–probe signals in the $(10, 10)_{100}$ SL quite similar to those in the $(10, 10)_{195}$ SL. In the $(10, 10)_{20}$ SL, both the 1C and 2C pump–probe signals show the oscillatory structures with the period of about 1.15 ps accompanying beats. The 1C pump–probe signal decays and almost disappears after about 80 ps, while the 2C pump–probe signal suddenly disappears at about 22 ps.

The 2C pump–probe signals in the $(10, 10)_{20}$ and $(10, 10)_{195}$ SLs will show the propagation of the phonon wavepacket generated near the surface of the SL sample. In the present 2C experiment, the penetration depth of the 360 nm pump light estimated from the absorption coefficient of $Al_{0.5}Ga_{0.5}As$ ($\sim 6.9 \times 10^5$ cm^{-1}) [13] is several tens nm and thinner than the total thicknesses of the $(10, 10)_{20}$ and $(10, 10)_{195}$ SLs that are 113 and 1104 nm, respectively. The phonon wave packet is generated near the surface region with the skin depth of several tens nm and propagates through the SL layer. The coherent oscillation signals will be observed in the propagation time of the phonon wavepacket through the SL layer, because the probe pulse with the wavelength of 720 nm detects the coherent signals throughout the SL layer. The sudden disappearance of the 2C pump–probe signal observed in the $(10, 10)_{20}$ SL implies the escape of the phonon wavepacket from the SL layer. The escape time calculated using the sound velocity of 5.2×10^5 cm s^{-1} for the SL is about 22 ps and in good agreement with the experimental result. In this calculation, the SL is regarded as an $Al_{0.5}Ga_{0.5}As$ alloy and the sound velocity is estimated by linear interpolation from those of GaAs and AlAs. On the other hand, the estimated escape time in the $(10, 10)_{195}$ SL is 210 ps, which leads to the fact that the 2C pump–probe signal hardly decays in the time region less than 100 ps as shown in figure 1. In the previous work [6], we reported the similar result for the propagation of the phonon wavepacket in the SL sample with a designed structure.

In order to analyse the coherent oscillation modes, we performed the FT of the time-domain signals as shown in figure 2. In the $(10, 10)_{195}$ SL, the 1C FT spectrum shows a strong central peak at 0.91 THz and two weak satellite peaks at 0.86 and 0.96 THz. On the other hand, the 2C FT spectrum shows two peaks of which frequencies are coincide with those of the two satellite peaks in the 1C FT spectrum. We have confirmed that the FT spectra of the $(10, 10)_{100}$ SL have the same profiles as those of the $(10, 10)_{195}$ SL. In the $(10, 10)_{20}$ SL, four

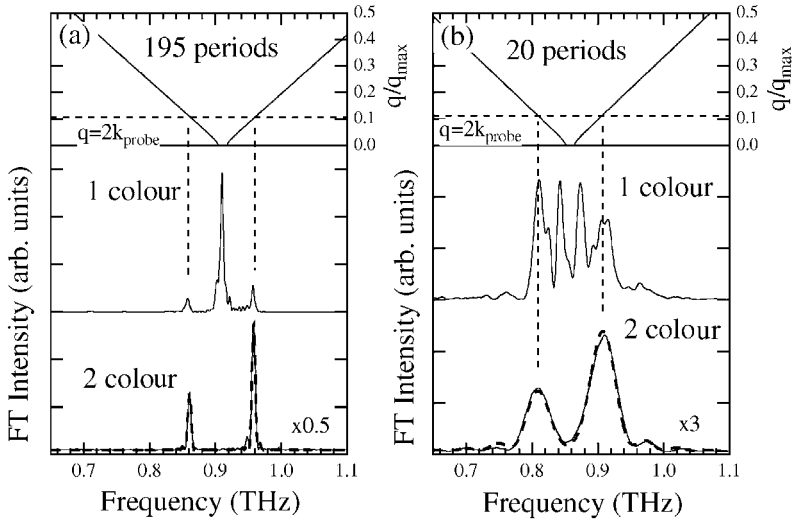

Figure 2. FT spectra of temporal traces in the (10,10) SLs with (a)195 and (b)20 periods, and dispersion curves of the FLA phonon calculated on the basis of an elastic continuum model. The dashed curves show the results fitted by using equation (2) in the text.

peaks in the 1C FT spectrum are observed at 0.81, 0.84, 0.87, and 0.91 THz, while the 2C FT spectrum shows two broad peaks at 0.81 and 0.91 THz. The intensities of the four peaks in the 1C FT spectrum are almost same. The centre frequencies of the two peaks observed in the 2C FT spectra of both the $(10, 10)_{195}$ and $(10, 10)_{20}$ SLs are slightly different. This frequency difference will be caused by the slight fluctuation of the constituent layer thicknesses.

The peak frequencies are compared with the dispersion curves of the FLA phonon in order to assign the peaks observed in the FT spectra. The dispersion curves of the FLA phonon were calculated on the basis of an elastic continuum model [14, 15] as depicted in figure 2. In the calculation, the constituent layer thicknesses are (10, 10) for the 195-periods SL and (11, 10) for the 20-periods SL. Here, $q_{\max}$ is the zone-edge wavevector π/D, and D is the period of SL. The horizontal broken lines show the wavevectors given by $q/q_{\max} = 2k_{\text{probe}}/q_{\max} = 4nD/\lambda$, where k_{probe} is the wavevector of the probe pulse and n is the refractive index at the wavelength λ of the probe pulse. We assume that the refractive index of the SL is the same as that of $Al_{0.5}Ga_{0.5}As$: $n = 3.4$ for 720 nm [13]. In the 2C FT spectra of the $(10, 10)_{195}$ and $(10, 10)_{20}$ SLs, the two peaks observed can be assigned to the FLA phonons with $q = 2k_{\text{probe}}$. In the 1C FT spectrum of the $(10, 10)_{195}$ SL, three peaks are attributed to the FLA modes at and near the zone centre. Group theory analysis indicates that the lower and upper branches of the doublet mode at the zone centre have A_1 and B_2 symmetries, respectively. Near the zone centre, the lower and upper branches have the symmetry of mixed A_1 and B_2 [15]. The B_2 mode at the zone centre in the 1C FT spectrum is not observed, while the A_1 mode at zone centre with the large intensity is observed. These results indicate that the coherent FLA phonons observed in the $(10, 10)_{195}$ SL are the Raman-active modes [4, 6]. In the 1C FT spectrum of the $(10, 10)_{20}$ SL, the two peaks at 0.84 and 0.87 THz correspond to the frequencies of the A_1 and B_2 modes at the zone centre, respectively, while the two peaks at 0.81 and 0.91 THz are assigned to the $q = 2k$ modes of the FLA phonon. Thus, the B_2 mode, which is forbidden in the SL with the infinite periodicity on the Raman scattering, appears by restricting the total thickness of the SL layer. The appearance of the B_2 mode at the zone centre is considered to be caused by the break

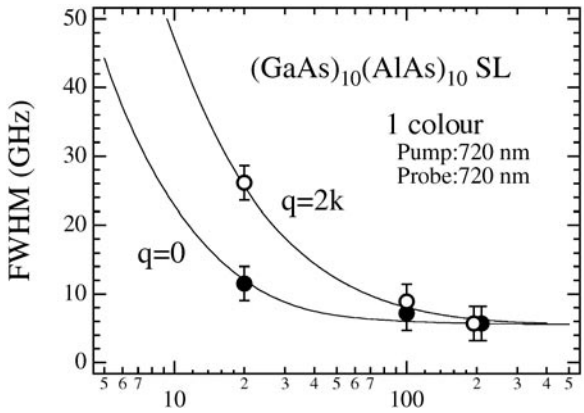

Figure 3. Theoretical and experimental values of FWHM of the FLA phonon obtained by using the 1C pump–probe technique as a function of total number of periods. The solid curves show the theoretical results.

of the mode symmetry due to the finiteness of the total thickness of the SL layer. This result is consistent with the result of MgO microcrystals obtained by using Raman spectroscopy [8].

In the 1C FT spectra shown in figure 2, the bandwidths of the FLA modes in the $(10, 10)_{20}$ SL are broader than those in the $(10, 10)_{195}$ SL. In the $(10, 10)_{20}$ SL, moreover, the bandwidths of the $q = 0$ modes are narrower than those of the $q = 2k$ modes. In microcrystals and SLs with the limited periodicity, finite-size effects on Raman scattering have been investigated [9–12]. The finite crystal size causes the relaxation of q-selection rule in Raman scattering, which induces the broadening of Raman peaks. We apply a theory of finite-size effects on Raman scattering [9–12] to the coherent phonons. The FLA phonon modes in the time-domain signals correspond to the phonon modes with the wave vector perpendicular to layers, and the finite size of SLs is limited to the growth direction (z direction) of the superlattice. Then we take only one dimension into consideration in this calculation. The intensity of the coherent phonon at the frequency ω can be written as

$$I(\omega) \propto \int_0^{\pi/D} \exp\left(-\frac{(q_z - q)^2(ND)^2}{4}\right) \frac{\mathrm{d}q_z}{[\omega - \omega(q_z)]^2 + (\Gamma_0/2)^2} \tag{1}$$

where $\omega(q_z)$ is a phonon dispersion relation, Γ_0 is an intrinsic bandwidth of coherent FLA phonon, and N is the total number of periods. Moreover, we phenomenologically use the Gaussian weight function for the Fourier coefficients in the calculation of the relaxation of q-selection rule [9–11]. Figure 3 shows the experimental and theoretical values of the full width at half maximum (FWHM) of the FLA phonon modes as a function of the total number of periods. The closed and open circles show the experimental results for the $q = 0$ and $2k$ modes, respectively, where the experimental values of the $q = 2k$ modes take the average values of FWHM for observed two peaks. The solid curves show the theoretical results for the $q = 0$ and $2k$ modes. The calculated FWHM is corrected by convolution of a instrumental transfer function and the line shape obtained from equation (1), where the fitted intrinsic bandwidth Γ_0 is 4.5 GHz and the instrumental bandwidth is 2.5 GHz corresponding to the window of the time delay. The value of Γ_0 was estimated from the observed bandwidth of figure 2(a). The calculated FWHM of the $q = 0$ mode is smaller than that of the $q = 2k$ mode. The difference in the bandwidths between the $q = 0$ and $2k$ modes will be explained as follows. When the relaxation of the q-selection rule occurs, the FLA phonon modes with $q = 2k$ will be broadened at the centre of $q = 2k$ according to the phonon dispersion. On the other hand,

because the phonon dispersion relation indicates the gap of the FLA phonon at $q = 0$ as shown in figure 2, the broadening of the FLA phonon modes with $q = 0$ will be suppressed due to the zone centre gap. Therefore, the broadening of the $q = 0$ modes is considered to be smaller than that of the $q = 2k$ mode. As shown in figure 3, the experimental results are in good agreement with the theoretical ones; accordingly, this indicates that the broadening of the coherent FLA phonon modes results from the relaxation of the q-selection rule induced by the finiteness of the periodicity.

In the 2C FT spectra, the $q = 2k$ modes in the $(10, 10)_{20}$ SL are much broader than those in the $(10, 10)_{195}$ SL. Moreover, in the $(10, 10)_{20}$ SL, the $q = 2k$ modes in the 2C FT spectrum are broader than those in the 1C FT spectrum. As mentioned above, the escape time of the wave packet from the $(10, 10)_{20}$ SL layer is shorter than that from the $(10, 10)_{195}$ SL layer. Therefore, the difference in the escape time will cause the difference in the bandwidth. In order to confirm this supposition, we have fitted a linear combination of two damped harmonic oscillations to the 2C pump–probe signals and subsequently performed the FT transform of the fitted results, using the following equation:

$$I(\omega) = \left| \int_0^{t_e} \sum_{j=1}^{2} A_j e^{-\gamma_j t} \cos(\omega_j t + \phi_j) e^{-i\omega t} \, dt \right|^2 \tag{2}$$

where t_e is the escape time from the SL layer, and A_j, γ_j, ω_j and ϕ_j are the oscillation amplitude, the decay rate, the characteristic frequency and the initial phase of the observed $q = 2k$ modes, respectively. The fitted FT spectra shown by the dashed curves in figure 2 are in good agreement with the experimental results. The values of fitting parameters obtained in the $(10, 10)_{20}$ SL are $A_1 = 1.5 \times 10^{-6}$, $\gamma_1 = 21$ GHz, $\omega_1 = 0.82$ THz, $\phi_1 = 121^\circ$, $A_2 = 2.0 \times 10^{-6}$, $\gamma_2 = 21$ GHz, $\omega_2 = 0.90$ THz and $\phi_2 = 163^\circ$. The agreement between the experimental and calculated results indicates that the bandwidth of the $q = 2k$ modes observed by the 2C pump–probe technique corresponds to the escape time t_e from the SL layer. Moreover, the decay rate γ in the $(10, 10)_{20}$ SL was obtained to be about 21 GHz by the fitting. This value is almost consistent with the bandwidth of the $q = 2k$ modes in the 1C FT spectrum. This result indicates that in the 2C FT spectrum of the $(10, 10)_{20}$ SL the broadening of the bandwidth due to the relaxation of the q-selection rule is hidden behind the escape time of the phonon wavepacket from the SL layer.

In summary, the coherent FLA phonons in the SL with the limited periodicity have been observed by using the reflection-type pump–probe technique. In the SL with the limited periodicity, we demonstrate the observation of the coherent FLA phonons with the B_2 symmetry at the Brillouin zone centre due to the break of the mode symmetry. The broadening of the bandwidth of the FLA phonon modes results from the relaxation of the q-selection rule induced by the finiteness of the total number of periods and the escape of the phonon wavepacket from the SL layer.

This work was partially supported by a Grant-in-Aid for the Scientific Research from the Ministry of Education, Culture, Sports, Science, and Technology of Japan.

References

[1] Dekorsy T, Cho G C and Kurz H 1999 *Light Scattering in Solids* vol 8, ed M Cardona and G Güntherodt (Berlin: Springer)
[2] Merlin R 1997 *Solid State Commun.* **102** 207
[3] Baumberg J J, Williams D A and Köhler K 1997 *Phys. Rev. Lett.* **78** 3358
[4] Mizoguchi K, Matsutani K, Hase M, Nakashima S and Nakayama M 1998 *Physica* B **249–51** 887

[5] Mishina T, Iwazaki Y, Masumoto Y and Nakayama M 1998 *Solid State Commun.* **107** 281
[6] Mizoguchi K, Hase M, Nakashima S and Nakayama M 1999 *Phys. Rev.* B **60** 8262
Mizoguchi K, Hase M, Nakashima S and Nakayama M 1999 *Physica* B **263–4** 48
[7] Bartels A, Dekorsy T, Kurz H and Köhler K 1998 *Appl. Phys. Lett.* **72** 2844
Bartels A, Dekorsy T, Kurz H and Köhler K 1999 *Phys. Rev. Lett.* **82** 1044
[8] Schlecht R G and Böckelmann H K 1973 *Phys. Rev. Lett.* **31** 930
[9] Nemanich R J, Solin S A and Martin R M 1981 *Phys. Rev.* B **23** 6348
[10] Richter H, Wang Z P and Ley L 1981 *Solid State Commun.* **39** 625
[11] Tiong K K, Amirtharaj P M, Pollak F H and Aspnes D E 1986 *Appl. Phys. Lett.* **44** 122
[12] Nakayama M, Kubota K, Kato H and Sano N 1986 *J. Appl. Phys.* **60** 3289
[13] Aspnes D E, Kelso S M, Logan R A and Bhat R 1986 *J. Appl. Phys.* **60** 754
[14] Rytov S M 1956 *Akust. Zh.* **2** 71 (Engl. transl. 1956 *Sov. Phys.–Acoust.* **2** 68)
[15] Jusserand B and Cardona M 1989 *Light Scattering in Solids* vol 5, ed M Cardona and G Güntherodt (Berlin: Springer)